Simulations of various configurations of the post-combustion CO₂ capture process applied to a cement plant flue gas: parametric study with different solvents

Lionel Dubois and Diane Thomas*

Chemical and Biochemical Process Engineering Unit, Faculty of Engineering, University of Mons, 20 Place du Parc, 7000 Mons, Belgium

Abstract

In order to reduce the operating costs of post-combustion CO_2 capture process by absorption-regeneration using amine based solvents for its application in the cement industry, the present study was focused on the Aspen Hysys™ simulation of different CO_2 capture process configurations (namely conventional configuration, "Rich Solvent Recycle" (RSR), "Solvent Split Flow" (SSF) and "Lean/Rich Vapor Compression" (L/RVC)) applied to the flue gas coming from the Norcem Brevik cement plant in Norway and using three different solvents, namely: monoethanolamine (MEA), piperazine (PZ) and piperazine-methyldiethanolamine (MDEA) blend. For each configuration and solvent, a parametric study was carried out in order to identify the specific operating conditions (flow rates ratio (L/G), split fraction, injection stage in the columns, flash pressure, etc.) minimizing the solvent regeneration energy and highlighting the energetical interest of such configurations. Energy savings of almost 30% were estimated with the RVC configuration and MDEA+PZ blend. A decrease of the condenser cooling energy was also noted. As perspectives, other configurations (such as InterCooled Absorber (ICA)) and combination of configurations will be considered in order to further reduce the energy consumption of the process. In addition to OPEX calculations, the consequence in terms of CAPEX of implementing each process configuration will have to be estimated for evaluating more precisely the global economic interest of using alternative process configurations for the application to cement plant flue gases.

* Corresponding author. Tel.: +32 65 37 44 04; fax: +32 65 37 44 07.
  E-mail address: diane.thomas@umons.ac.be

Nomenclature

A	[m²]	transfer area
$E_{condenser}$	[GJ/t_{CO2}]	condenser cooling energy
$E_{LVC/RVC}$	[GJ/t_{CO2}]	LVC/RVC compression energy
E_{pumps}	[GJ/t_{CO2}]	pumping energy
E_{regen}	[GJ/t_{CO2}]	solvent regeneration energy
G	[m³/h]	volumetric gas flowrate
$G_{CO2,capt}$	[t_{CO2}/h]	mass flow rate of captured (produced) CO_2
L	[m³/h]	liquid flowrate
U	[kJ/h m² °C]	heat transfer coefficient
$y_{CO2,in}$	[vol.%]	CO_2 content in the gas to treat (inlet of the absorber)
$\alpha_{CO2, rich/lean}$	[mol_{CO2}/mol_{amine}]	CO_2 loading of the rich/lean solution
Φ_{boiler}	[GW]	reboiler duty provided for the regeneration

1. Introduction

Even if Carbon Capture Storage and Utilization (CCSU) has gained widespread attention as an option for reducing greenhouse gas emissions from power plants, specific developments are still needed for the application to other sectors, specifically for the cement industry where the flue gas has a higher CO_2 content in comparison with power plants ones. More precisely, the post-combustion CO_2 capture process by absorption-regeneration using amine based solvents (represented on Fig. 1) is the more mature technology for the application in the cement industry but it is still needed to reduce its energetic costs, especially for the solvent regeneration step.
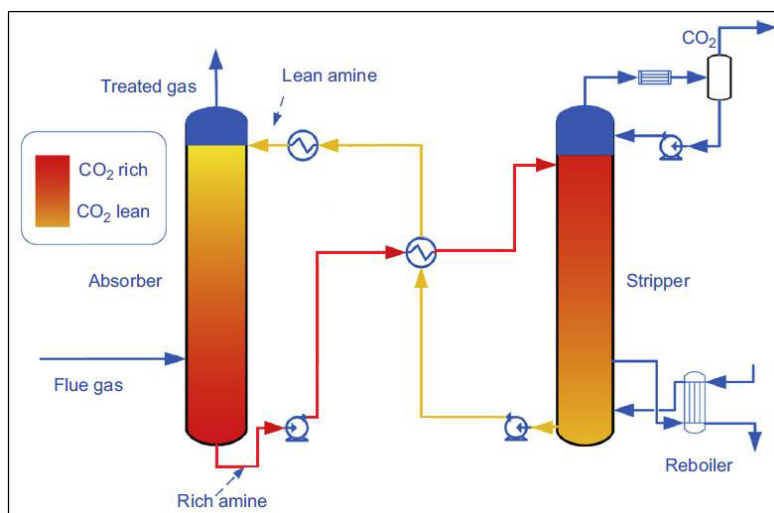

Fig. 1. Conventional amine-based CO_2 capture absorption-regeneration process (adapted from [1])

In this context, the present study is focusing on the simulation of different CO_2 capture process configurations [2], namely, compared to the conventional process configuration, the "Rich Solvent Recycle" (RSR), the "Solvent Split Flow" (SSF), and the "Lean/Rich Vapor Compression" (L/RVC) configurations. These simulations were applied to the flue gas coming from the Norcem Brevik cement plant (Norway) where different post-combustion CO_2 capture technologies were tested [3] and especially the absorption-regeneration process (Aker Solutions technology) in a quite conventional configuration (including only an Aker's property energy savings system). For each configuration considered in our study, in addition to the flow rates ratio (L/G) (optimized for all the configurations), a parametric

study was carried out in order to identify the specific operating conditions (split fraction, injection stage in the columns, flash pressure, etc.) minimizing the solvent regeneration energy (E_{regen}) and allowing to highlight the interest of using alternative process configurations in order to reduce the energy consumption of the process. The simulations were carried out considering the design of a pilot unit used during a previous European project, namely the CASTOR/CESAR one [4]. In a first step, these simulations were performed with the benchmark monoethanolamine (MEA) 30 wt.% as solvent but in a second step, other interesting solvents (piperazine (PZ) and activated methyldiethanolamine (aMDEA)) were also studied and the energy savings obtained with the different solvents and configurations were compared.

Note that the full details regarding the optimization works in relation with the different solvents and configurations considered in the present study are available in [5].

2. Aspen Hysys^{TM} simulations of the absorption-regeneration CO₂ capture process

2.1. Modeling parameters

The simulation of the absorption-regeneration process was developed in Aspen Hysys^{TM} v.8.8 software using the Acid Gas Package and the "Efficiency calculation mode". This package was specifically developed for simulating the removal of acid gases (CO_2 and H_2S). It includes the physicochemical properties of these acid gases, water, amines alone (such as MEA and PZ) and also several mixtures (such as MDEA+PZ). The Acid Gas Property Package is based on extensive developments in rate-based, chemical absorption process simulation and molecular thermodynamic models for aqueous amine solutions [6]. The thermodynamic models used in the package are the Electrolyte Non-Random Two-Liquid (eNRTL) activity coefficient model for electrolyte thermodynamics in liquid phase [7] and the Peng-Robinson equation of state for the vapor phase. The property package contains the eNRTL model parameters, physical property data for aqueous amine solutions and other transport property model parameters [8-9].

As indicated in Tab.1, in addition to the dissociation reactions (reactions (1) to (4)) considered for all the solvents, specific reactions are included in the Acid Gas Package depending on the solvent selected for the simulation (reaction (5) to (7) for MEA, (8) to (13) for PZ and (14) to (16) for MDEA). In the case of PZ-MDEA blend, reactions related to both solvents are taken into account in the calculations.

Table 1. Acid Gas Package reactions for water dissociation, MEA ($HO(CH_2)_2NH_2$), PZ ($C_4H_8(NH)_2$) and MDEA ($CH_3N(CH_2CH_2OH)_2$)

	N°	Reaction	Type
H_2O + CO_2	(1)	$2\ H_2O \leftrightarrow H_3O^+ + OH^-$	Equilibrium
	(2)	$H_2O + HCO_3^- \leftrightarrow H_3O^+ + CO_3^{2-}$	Equilibrium
	(3)	$CO_2 + OH^- \rightarrow HCO_3^-$	Kinetic
	(4)	$HCO_3^- \rightarrow CO_2 + OH^-$	Kinetic
MEA	(5)	$HO(CH_2)_2H^+NH_2 + H_2O \leftrightarrow HO(CH_2)_2NH_2 + H_3O^+$	Equilibrium
	(6)	$HO(CH_2)_2NH_2 + H_2O + CO_2 \rightarrow HO(CH_2)_2NHCOO^- + H_3O^+$	Kinetic
	(7)	$HO(CH_2)_2NHCOO^- + H_3O^+ \rightarrow HO(CH_2)_2NH_2 + H_2O + CO_2$	Kinetic
PZ	(8)	$C_4H_8(NH)_2 + H_3O^+ \leftrightarrow H_2O + C_4H_8(NH)_2H^+$	Equilibrium
	(9)	$C_4H_8(NH)_2\ HCOO + H_2O \leftrightarrow C_4H_8(NH)_2\ COO^- + H_3O^+$	Equilibrium
	(10)	$C_4H_8(NH)_2 + H_2O + CO_2 \rightarrow C_4H_8(NH)NCOO^- + H_3O^+$	Kinetic
	(11)	$C_4H_8(NH)NCOO^- + H_3O^+ \rightarrow C_4H_8(NH)_2 + H_2O + CO_2$	Kinetic
	(12)	$C_4H_8(NH)NCOO^- + H_2O + CO_2 \rightarrow C_4H_8(NCOO^-)_2 + H_3O^+$	Kinetic
	(13)	$C_4H_8(NCOO^-)_2 + H_3O^+ \rightarrow C_4H_8(NH)NCOO^- + H_2O + CO_2$	Kinetic
MDEA	(14)	$CH_3N(CH_2CH_2OH)_2 + H_3O^+ \leftrightarrow H_2O + CH_3N(CH_2CH_2OH)_2H^+$	Equilibrium
	(15)	$CH_3N(CH_2CH_2OH)_2 + H_2O + CO_2 \rightarrow CH_3N(CH_2CH_2OH)_2H^+ + HCO_3^-$	Kinetic
	(16)	$CH_3N(CH_2CH_2OH)_2H^+ + HCO_3^- \rightarrow CH_3N(CH_2CH_2OH)_2 + H_2O + CO_2$	Kinetic

The installation simulated in the present work was based on [10] (CASTOR/CESAR pilot unit) because all the design and operating parameters in relation with this unit are available which is not the case with most of the other installations. This pilot is sized to handle a flow of 4000 Nm³/h at the inlet of the absorber after removal of a large

portion of water, cooling and compression. The dimensions of the absorber and the stripper, and the operating conditions in each column are given in Table 2. The flowsheet developed in Aspen Hysys[TM] is illustrated on Fig. 2 for the case of MDEA+PZ as solvent.

Table 2. Dimensions and operating conditions of the columns

	Absorber	Stripper
Column Diameter [m]	1.1	1.1
Packing height [m]	17 (17 stages of 1 m)	10 (10 stages of 1 m)
Packing type	Random packing IMTP 50	Random packing IMTP 50
Inlet liquid temperature [°C]	40	110
Bottom pressure [kPa]	120	200
Specific pressure drop [kPa/m]	0.5	0.5

The composition of the gas to treat ($y_{CO2,in}$ around 20%) was based on the Brevik cement plant flue gas in Norway. The gas is initially at 165°C and 100 kPa prior to compression to 120 kPa and cooling down to 40°C before entering the absorber (see conditioned gas composition in Tab. 3). After conditioning (not represented on Fig. 2), the gas enters the absorber and contacts counter-currently the amine based solvent.
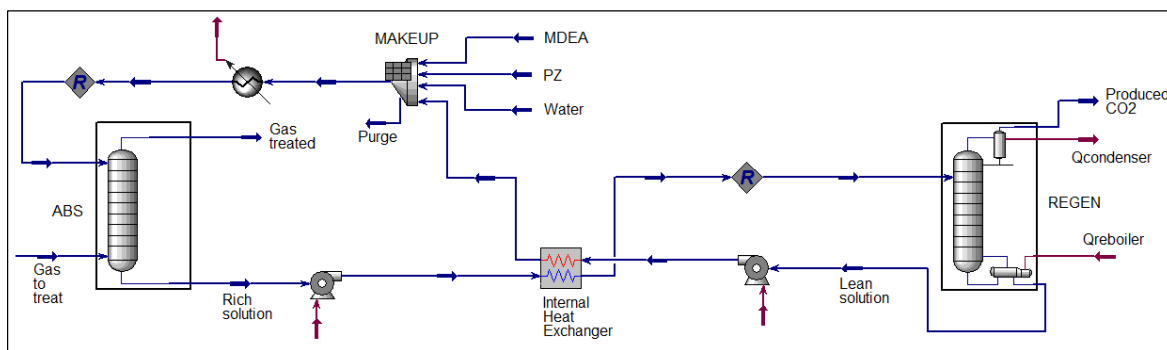

Fig. 2. Aspen Hysys[TM] flow sheet for the conventional process configuration (illustration for MDEA+PZ)

The amount of CO_2 absorbed into the column is calculated using the "rate-based model". At the outlet of the column, the "Rich solution" is pumped and preheated to 110°C thanks to the internal heat exchanger (corresponding to a pinch of around 10°C at the hot side of the exchanger). Then, into the regeneration column, the gas is stripped thanks to the heating power and the CO_2 is recovered at the top of the regeneration column ("produced CO_2" in the flow sheet).

Table 3. Composition (mol. fraction) of the gas to treat (G = 4000 m³/h, 40°C, 120 kPa) after conditioning

N_2	0.647	CO	1.33 10^{-3}
CO_2	0.204	SO_2	1.11 10^{-4}
H_2O	0.062	NO	4.74 10^{-4}
O_2	0.086	NO_2	1.77 10^{-6}

The regeneration occurs at 200 kPa (for MEA) or 600 kPa (for PZ-based solvents) and at the solvent boiling point (for example around 120°C for an aqueous solution of MEA 30 wt.% at such pressure level). Two operating parameters are automatically adjusted in order to satisfy two conditions: the reboiler duty, which is adapted in order to recover the CO_2 amount targeted for the simulation (corresponding to an absorption ratio equal to 90 % meaning

that 90% of the molar flow rate of CO_2 entering the absorption column is recovered at the outlet of the regeneration column), and the condenser cooling energy, which is adjusted to meet the CO_2 purity specification (98 mol.% in the present study).

The regenerated solvent ("lean solution") which still contains some CO_2 is then pumped through the heat exchanger in order to be cooled down. A makeup unit is added in order to automatically adjust the total flow of liquid while reaching the desired concentration of amine. Note that this makeup unit ensures the water and solvent balances (both in MDEA and PZ on Fig. 2) and compensates possible losses in amine and water at the outlet of the absorber and regenerator. After the makeup unit, the lean solution is cooled down to 40°C before entering in the absorption column and beginning a new absorption-regeneration cycle. The washing section at the top of the absorber in the real installation was not simulated in the present work as it does not influence the absorption-regeneration global performances.

2.2. Process configurations simulated

Three categories of process improvements were studied in the present work, namely: the absorption enhancement, the exergetic (or heat) integration and the heat pump effect. A lot of information regarding such process modifications are available in [11] and all the details regarding the precise configurations simulated in the present study are available in [5]. A summary of the objective and principle of each process modification is given in Tab. 4.

Table 4. Objective and principle of each process modification simulated in the present study

Category	Name	Objective	Principle
Absorption enhancement	Rich Solvent Recycle (RSR)	Increasing the CO_2 loading at the absorber bottom (reducing excessive driving force in the absorber section).	A part of the rich solution coming from the absorber bottom is recycled into the absorber.
Exergetic (or heat) integration	Solvent Split Flow (SSF)	Performing heat integration between the different process streams in order to reduce the heat losses and the solvent regeneration energy.	A part of the rich solution coming from the absorber bottom is directly sent at the top of the regeneration column without being preheated by the internal heat exchanger.
Heat pump effect	Lean Vapor Compression (LVC)	Increasing the heat quality provided to the system thanks to the valorization of heat available in the process at a low quality level in order to reduce the reboiler steam demand.	The lean or rich solvent is flashed in order to produce a gaseous stream (mainly composed of water and carbon dioxide) which is compressed and sent to the stripper.
	Rich Vapor Compression (RVC)		

For each configuration, Tab. 5 gives the operating parameters that were optimized in order to minimize the energy consumption of the process, especially the specific solvent regeneration energy. The flowsheet modifications associated with each process configuration are represented on Fig. 3.

Regarding the RSR modification, it must be noted that the rich solution going back to the column is generally cooled down in order to promote the CO_2 absorption. Concerning the SSF configuration (also called "Rich Solvent Splitting"), it leads to a modification of the temperature profile into the stripper (it is more smoothed than with conventional configuration) and the heat recovered from hot lean solvent is maximized.

Table 5. Operating parameters that was optimized for each process configuration

Type of variable	Conventional	RSR	SSF	LVC	RVC
Flow rate ratio	(L/G)	(L/G)	(L/G)	(L/G)	(L/G)
Level	Injection level into the stripper	Re-injection level into the absorber	Injections level of the cold solution into the stripper Injections level of the preheated solution into the stripper	-	-
Temperature	-	Re-injection temperature into the absorber		-	-
Flow fraction	-	Re-injected fraction	Split fraction	-	-
Pressure	-	-	-	Flash pressure	Flash pressure

Furthermore, thanks to the cold solution injected at the top of the stripper, the condenser cooling energy is reduced. Moreover, for a defined heat exchanger, splitting the rich solution with SSF will change the liquid flow rate inside this exchanger leading to a modification of the temperature of the rich solution at its outlet. In order to correctly simulate the internal heat exchanger, as used for example in [12], the product "UA [kJ/°C h]" of the heat transfer coefficient (U [kJ/h m² °C]) and area (A [m²]) corresponding to the base case is considered as design parameter.
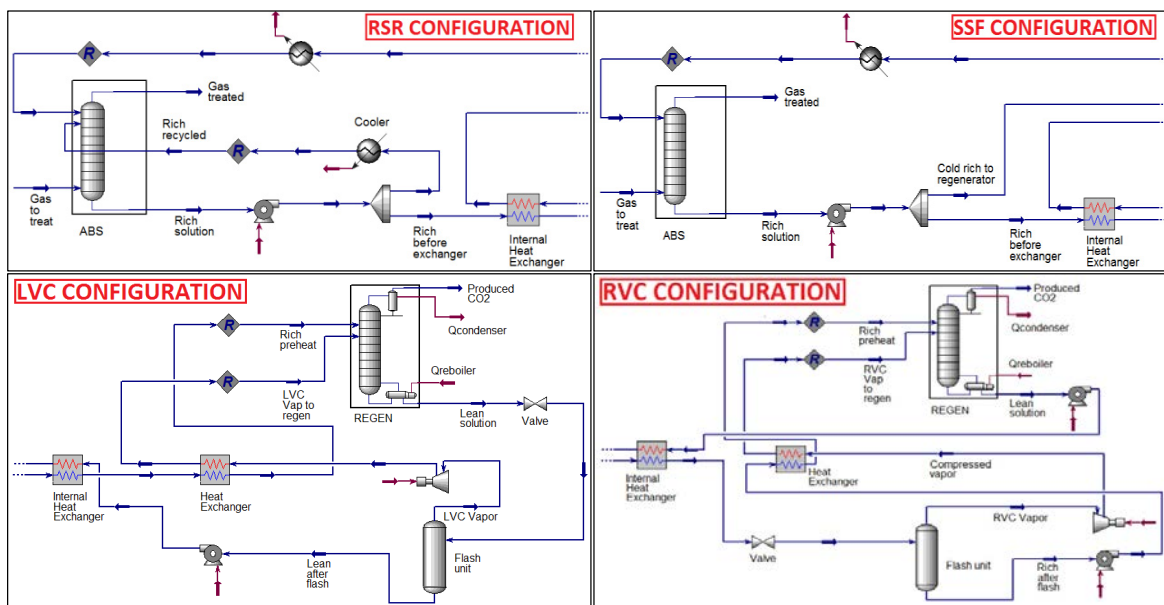

Fig. 3. Focus on the modifications of the Aspen Hysys™ flow sheet for each alternative configuration

With respect to L/RVC configurations, such a process modification reduces the reboiler steam demand and reduces the temperature at the top of the stripper which also decreases the cooling requirement in the condenser.

Based on operational experiences such as in [10], this modification is generally accompanied with an expansion of the internal heat exchanger in order to reduce the hot pinch of this exchanger to 5°C. Moreover, as the vapor coming from the compressor installed after the flash unit is very hot (which could lead to a hot spot inducing degradation problems into the bottom of the stripper), a supplementary heat exchanger is installed in order to cool down this vapor while giving a preheating complement to the rich solution before entering the regeneration column.

As a conclusion, it was shown that four different configurations are considered in the present work, namely RSR, SSF, LVC and RVC, corresponding to the three categories of process modifications. These configurations were selected because in practice they should not imply too much modifications of the conventional process and some of them (such as LVC) have already shown interesting results for the application to power plants, which has to be confirmed here for the application to cement plants.

2.3. Modeling specificities for each solvent

The three solvents selected in this study are: monoethanolamine (MEA), piperazine (PZ) and piperazine-methyldiethanolamine (PZ+MDEA) blend. Depending on the chosen solvent, some parameters had to be adapted in order to carry out realistic simulations. Concerning the primary amine MEA, the conventional solvent concentration is 30 wt.% and as this solvent was used in the industrial pilot installation simulated, no adaptations of the operating conditions were necessary. Regarding the cyclical diamine PZ, its concentration was fixed at 40 wt.% (8 M) and the regeneration pressure was increased from 200 kPa (for MEA 30 wt.%) to 600 kPa (final pressure value kept for the performances comparisons with other solvents in order to regenerate the solvent at 150°C). These conditions were based on literature [13-14].

Finally, for the PZ-MDEA blend, several studies (such as [15-16]) indicated that the total amine concentration in the solvent used in the CO_2 capture process is around 50 wt.% (different proportions between PZ and MDEA are possible) and with pressure of 25-40 bars and 2-5 bar for the absorption and regeneration respectively. Nevertheless, in the present case, in order to make realistic comparisons between the three solvents considered, the simulations were carried out with the same design and operating parameters as for PZ 40 wt.% (pressure levels in the columns and total amine concentration). The optimum PZ/MDEA proportion was identified to be MDEA 10 wt.% + PZ 30 wt.% thanks to preliminary simulations presented in [5].

3. Aspen Hysys^{TM} simulations results

First of all, it must be noted that the simulation method applied in the present study was previously validated with the use of [10] results (application to power plant) and also with the use of another study (other pilot design but applying same modeling method) concerning the application to a cement plant (see [17] for more details).

Globally, the objective of the simulation works was to minimize the solvent regeneration energy (E_{regen}) [GJ/t_{CO2}] defined as:

$$E_{regen} = \frac{\Phi_{boiler}}{G_{CO2,capt}}$$ (1)

where Φ_{boiler} [GJ/s] is the energy provided for solvent regeneration in the reboiler and $G_{CO2,capt}$ [t_{CO2}/s] is the produced CO_2 rate (98 mol.% purity) recovered at the outlet of the regeneration column (corresponding to an absorption ratio equal to 90 mol.%.).

It must be noted that in accordance with ECRA (European Cement Research Academy), no compression of the produced CO_2 is considered in the present study because the focus is put on CO_2 valorization options for which the level of CO_2 compression can be different depending on the CO_2 conversion process envisaged. Moreover, as some

configurations imply the optimization of several operating parameters, systematic parametric studies were carried out in order to identify the realistic conditions leading to a minimum of E_{regen}. Firstly, each operating parameter was varied separately and secondly, cross-variations were carried out with the aim of identifying the operating parameters minimizing E_{regen}. The present paper considers MEA 30wt.% as reference for illustrating the simulation results obtained with the different configurations and a summary of the results obtained with the three solvents is given in sections 3.5 and 3.6. More details on the parametric study carried out with the three solvents are available in [5].

3.1. Conventional process configuration

The first operating parameter that must optimized for each process configuration in order to minimize E_{regen} is the (L/G) ratio. The simulated results for different (L/G) ratios (varying the liquid flow rate due to the fact that the gaseous flow rate was kept constant) are presented on Fig.4. The trend of this graph is quite typical for such process and allows to identify the (L/G) minimizing E_{regen}, namely 5.56 10^{-3} (liquid flow rate of 22 m³/h) leading to E_{regen} equal to 3.36 GJ/t_{CO2}. This value is in the range of conventional values measured with MEA 30 wt.% for power plants (between 3 and 4 GJ/t_{CO2}, see for example [10]).
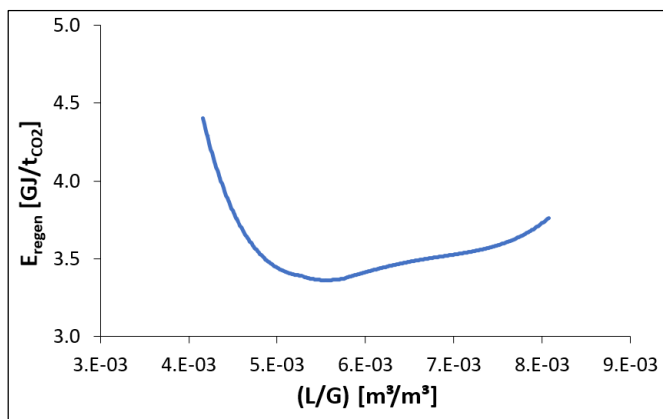

Fig. 4. Regeneration energy as a function of the (L/G) ratio for the conventional configuration with MEA 30 wt.%

Nevertheless, it must be emphasized that 3.36 GJ/t_{CO2} is close to the minimum values conventionally measured for MEA 30 wt.% which could be justified by the fact that a higher CO_2 content in the gas to treat (20 vol.% for the cement plant considered in the present case in comparison with the range 5-15 vol.% for power plants) is favourable to the absorption process even if the maximum temperature reached into the absorber (around 85°C) is a little bit higher than other values (75-80°C) generally measured. This is linked to a higher CO_2 content which induces a higher heat of reaction. The implementation of absorber intercooling seems a good option to be envisaged in the future to even more taking advantage of high $y_{CO2,in}$. The results corresponding to the optimal operating conditions with MEA 30 wt.% are provided in Tab. 6 and Tab. 7.

Table 6. Simulation results for the base case with MEA 30 wt.% ((L/G) = 5.56 10^{-3} m³/m³)

Parameter	Value
E_{regen}	3.36 GJ/t_{CO2}
$E_{condenser}$	-1.90 GJ/t_{CO2}
E_{pumps}	1.57 10^{-2} GJ/t_{CO2}
$\alpha_{CO2,rich}$	0.506 mol CO_2/mol MEA
$\alpha_{CO2,lean}$	0.211 mol CO_2/mol MEA

In addition to the regeneration energy already commented, it can be seen in Tab. 6 that even if it is not an issue for the absorption-regeneration process, the condenser cooling energy ($E_{condenser}$) is significant (-1.90 GJ/t$_{CO2}$) and reducing it thanks to the use of alternative configurations would be also benefic in practice (reduction of the water flow rate circulating into the condenser). Regarding the consumption of the liquid pumps (E_{pumps}) equal to $1.57 \ 10^{-2}$ GJ/t$_{CO2}$, it corresponds to only ≈ 0.5 % of the regeneration energy and is thus not significant for the evaluation of the overall energy consumption of the process. Regarding the CO_2 loadings values for the rich ($\alpha_{CO2,rich}$) and the lean ($\alpha_{CO2,lean}$) solutions, they are equal respectively to 0.506 and 0.211 mol CO_2/mol MEA, quite typical values for MEA 30 wt.% even if it must be noted that the value slightly higher than 0.5 is possible thanks to the CO_2 content of the gas to treat (≈ 20 mol.%).

Table 7. Gaseous compositions for the base case with MEA 30 wt.% ((L/G) = $5.56 \ 10^{-3}$ m³/m³) in mol. fraction

Component	Gas to treat	Gas treated	Produced CO_2
N_2	$6.47 \ 10^{-1}$	$6.29 \ 10^{-1}$	$1.54 \ 10^{-4}$
CO_2	$2.04 \ 10^{-1}$	$2.09 \ 10^{-2}$	$9.80 \ 10^{-1}$
H_2O	$6.21 \ 10^{-2}$	$2.64 \ 10^{-1}$	$1.95 \ 10^{-2}$
O_2	$8.56 \ 10^{-2}$	$8.33 \ 10^{-2}$	$3.72 \ 10^{-5}$
CO	$1.33 \ 10^{-3}$	$1.30 \ 10^{-3}$	$4.48 \ 10^{-7}$
SO_2	$1.11 \ 10^{-4}$	$5.35 \ 10^{-5}$	$2.98 \ 10^{-4}$
NO	$4.74 \ 10^{-4}$	$4.61 \ 10^{-4}$	$4.45 \ 10^{-6}$
NO_2	$1.77 \ 10^{-6}$	$4.18 \ 10^{-7}$	$7.13 \ 10^{-6}$
MEA	-	$3.77 \ 10^{-4}$	$7.65 \ 10^{-11}$

Concerning the gaseous compositions of the gas treated gas and the produced CO_2 given in Tab. 7, as no specific reactions were added concerning the other gaseous species (SO_2, NO, NO_2, etc.), the decrease of their concentrations into the absorber can only be associated to their solubilization into the liquid phase. Regarding the MEA, only very small quantities are present into the treated gas and the produced CO_2. These results confirm the absorption ratio of 90% fixed as simulation parameter, and also the fact that the produced CO_2 contains 98 mol.% of CO_2, the rest being mainly composed of water.

To conclude the analysis of this base case, it has to be highlighted that the presented results were obtained for a rich solution injected at stage 9 into the stripper. Indeed, it was found that injecting at level 9 or level 10 (top of the column) gives similar results in terms of regeneration energy while the condenser cooling energy is a little bit lower when the rich solution is not injected too close to the condenser, namely at stage 9.

3.2. Rich Solvent Recycle (RSR) configuration

The influence of the re-injected solution temperature on the process performances was investigated and is illustrated on Fig. 5 for MEA 30 wt.%, considering a liquid flow rate of 24 m³/h (corresponding to the optimum value of (L/G) identified for RSR configuration), 35% of solution re-injection into the stripper at stage 4. The effect of cooling the re-injected solution is presented in terms of regeneration energy and rich CO_2 loading. As expected by an absorption enhancement process modification as RSR, the recirculation into the absorber of a cooled solution allows to increase the CO_2 loading of the rich solution (from 0.507 to 0.520 mol CO_2/mol MEA in the presented case when the solution is cooled down from 50°C to 5°C) leading to a decrease of the regeneration energy from 3.15 to 2.95 GJ/t$_{CO2}$. As cooling the solution to a too low level would be unfavorable in terms of cooling energy, it seems more feasible in practice to consider the cooling of the solution to 40°C (same temperature of the solution at the top of the absorber), which will be considered as reference for the results comparison between the different solvents and configurations.

Two other parameters were also optimized, namely the volume split fraction and the re-injection stage of the

cooled rich solution re-injected into the absorber. The results of the parametric study carried out on these parameters for MEA 30 wt.% are presented on Fig. 6 (a) and Fig. 6 (b). Note that each graph is presented considering the optimum values of the other operating parameters.
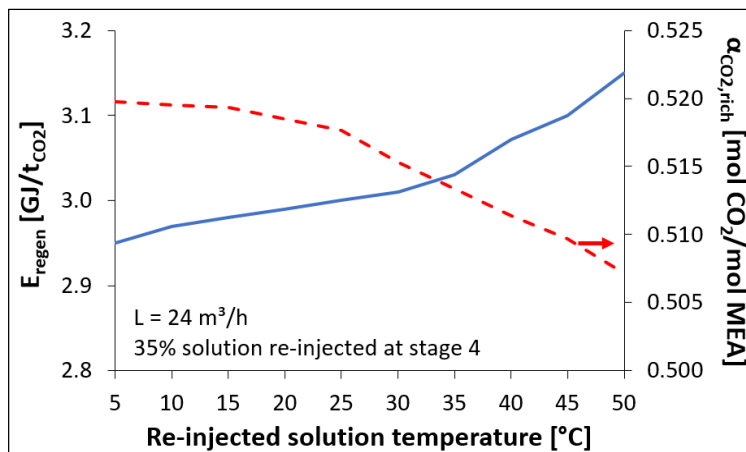

Fig. 5. E_{regen} and $\alpha_{CO2,rich}$ as a function of the re-injected solution temperature into the absorber (35% re-injection at stage 4) – RSR configuration with MEA 30 wt.%

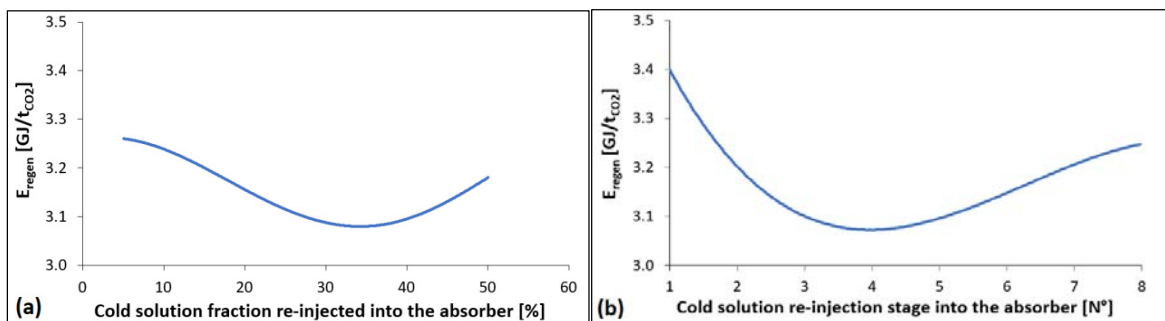Fig. 6. E_{regen} as a function of the volume fraction (a) and re-injection stage (b) of the re-injected solution into the absorber – RSR configuration with MEA 30 wt.%

It can be seen on Fig. 6 (a) that the optimum value of the split fraction for MEA 30 wt.% is 35% and on Fig. 6 (b) that re-injecting the cold solution in the absorber at stage 4 leads to the minimum of E_{regen}, namely 3.07 GJ/t_{CO2}, corresponding to energy savings of 8.5% in comparison with the conventional process configuration. The results of the optimization study for RSR configuration with the different solvents and the simulations results associated are globally summarized in sections 3.5 and 3.6.

3.3. Solvent Split Flow (SSF) configuration

As indicated previously, three operating parameters must be optimized with the "Solvent Split Flow" (SSF) configuration, namely the (L/G) ratio (identified to 5.81 10^{-3} for MEA 30 wt.%), the fraction of the rich solution ("cold fraction") which is injected without being preheated and the re-injection level of the preheated solution into the regeneration column. It must be noted that the cold solution is conventionally injected at the top of the stripper (stage 10) in order to reduce the condenser cooling energy.

Fig. 7 (a) and Fig. 7 (b) show, for MEA 30 wt.%, the influence on E_{regen} of the different operating parameters linked to SSF configuration. As for RSR configuration, each graph is presented considering the optimum values of the other operating parameters, such as (L/G) ratio. It can be seen on Fig. 7 (a) that the optimum split fraction of the cold solution is 26 vol.% and on Fig. 7 (b) that E_{regen} is minimized for a hot rich solution injected into stripper at stage 7. This graph also confirms the interest of injecting the cold solution at the top of the stripper (stage 10).
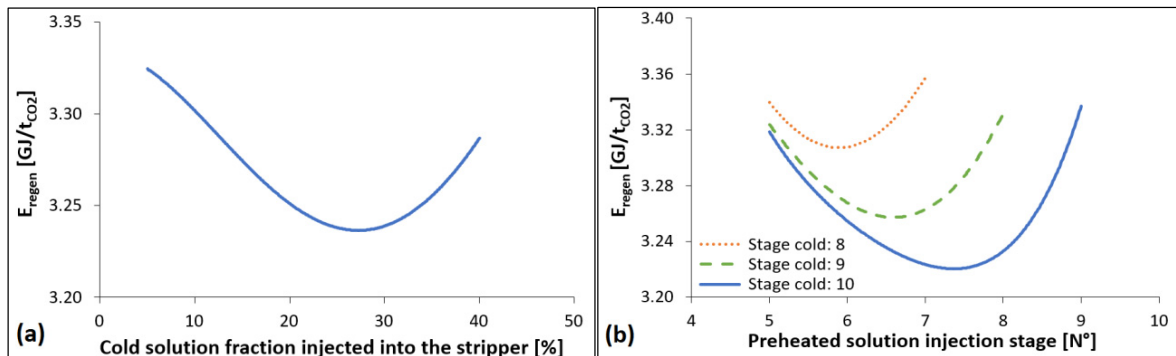

Fig. 7. E_{regen} as a function of the volume fraction of the cold solution (a) and of the re-injection stage of the hot and cold solutions (b) into the stripper – SSF configuration with MEA 30 wt.%

Globally, the optimum value of E_{regen} with MEA 30 wt.% is equal to 3.22 GJ/t_{CO2}, which means 4.2% energy savings in comparison with the conventional configuration. The results of the optimization study for SSF configuration with the different solvents and the simulations results obtained with the optimal operating conditions are globally summarized in sections 3.5 and 3.6.

3.4. Lean Vapor Compression (LVC) and Rich Vapor Compression (RVC) configurations

In addition to the (L/G) ratio (optimum values of 5.30×10^{-3} and 7.33×10^{-3} for LVC and RVC configurations respectively), the main operating parameter that must be defined for LVC and RVC configurations is the flash pressure variation (Δp). As illustrated on Fig.8, despite the decrease of the temperature of the rich solution at the outlet of the internal heat exchanger (for example, a decrease of almost 20°C was observed with MEA 30 wt.% in comparison with the conventional configuration), a higher LVC/RVC flash pressure leads to a quasi linear decrease of the regeneration energy.
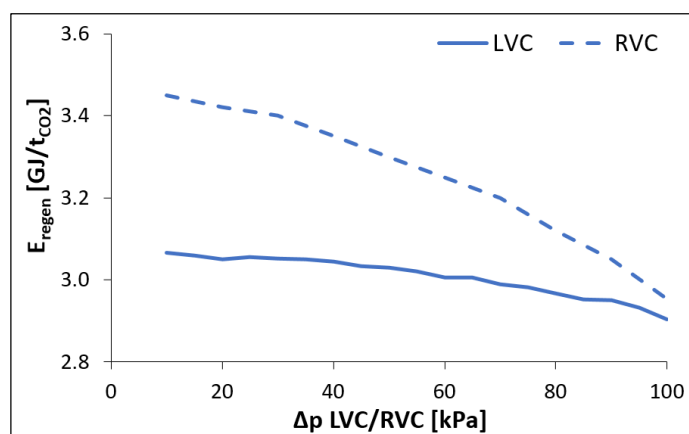

Fig. 8. E_{regen} as a function of the Δp – LVC/RVC configurations with MEA 30 wt.%

This can be observed for all solvents even if it is more pronounced with PZ and MDEA+PZ than with MEA 30 wt.% due to the fact that these solvents were regenerated at a higher pressure (600 kPa) than MEA 30 wt.% (200 kPa) allowing a larger Δp. Moreover, even if due to the flash unit the temperature of the rich solution at the outlet of the internal heat exchanger is decreased, another heat exchanger gives a complementary preheating to the rich solution (from 2 to 5°C) thanks to its heat exchange with the hot vapor coming from the vapor compression unit.

Thanks to LVC and RVC configurations, the MEA 30 wt.% regeneration energy is decreased to 2.91 and 2.95 GJ/t$_{CO2}$, which corresponds to a decrease of around 13% of E$_{regen}$ in comparison with the base case configuration. The results of the optimization study for LVC configuration with the different solvents and the simulations results associated are globally summarized in sections 3.5 and 3.6.

3.5. Summary of the parametric study results for the three solvents

The results of the parametric study carried out for the three solvents MEA 30 wt.%, PZ 40 wt.% and MDEA 10 wt.% + PZ 30 wt.% with the different process configurations are presented in Tab. 8.

Table 8. Optimum operating conditions for each process configuration and solvent

(L/G) [m³/m³]	CONV. conf.	RSR conf.	SSF conf.	LVC conf.	RVC conf.
MEA	5.56 10^{-3}	6.06 10^{-3}	5.81 10^{-3}	5.30 10^{-3}	7.33 10^{-3}
PZ	3.16 10^{-3}	3.54 10^{-3}	4.55 10^{-3}	6.07 10^{-3}	6.57 10^{-3}
MDEA+PZ	3.04 10^{-3}	3.04 10^{-3}	4.03 10^{-3}	3.54 10^{-3}	3.54 10^{-3}

RSR conf.	Split fraction rich sol. [%]	Re-injection sol. temp. [°C]	Re-injection abs. stage [N°]		SSF conf.	Split fraction rich sol. [%]	Preheated sol. stripper stage [N°]	Cold sol. stripper stage [N°]
MEA	35	40	4		MEA	26	7	10
PZ	30	40	3		PZ	15	6	10
MDEA+PZ	40	40	3		MDEA+PZ	15	3	10

LVC/RVC conf.	LVC Flash Δp [kPa]	RVC Flash Δp [kPa]
MEA	100	100
PZ	500	500
MDEA+PZ	500	500

First of all, concerning the (L/G) ratio, some differences are observed between the different solvents and configurations. For example, the optimum (L/G) ratio with MDEA + PZ using RSR configuration (3.04 10^{-3}) is almost the half of the MEA one with the same configuration. For all the solvents, the optimum (L/G) is higher with the RVC configuration than with the conventional one.

Regarding the other parameters, some similarities are observed. Indeed, for the RSR configuration, the optimum split fraction of the rich solution is between 30 and 40% for the three solvents. This split fraction is 15% for PZ-based solvents considering SSF configuration but it is higher with MEA (namely 26%). Concerning the optimum injection stages, the main difference is observed for MDEA+PZ with SSF configuration, the hot solution injection stage being N°3 for this solvent and N°6 or N°7 for PZ or MEA respectively. Finally, for the LVC and RVC configurations, it was shown that considering the maximum pressure (Δp equal to 100 kPa for MEA and 500 for PZ-based solvents) leads to the minimum of E$_{regen}$.

The simulation results obtained with these optimum parameters for the different solvents and configurations are compared in section 3.6.

3.6. Global comparison of the simulation results with the different solvents and configurations

The simulation results obtained with the different solvents and configurations are provided in Tab. 9.

Table 9. Summary of the simulation results for each process configuration and solvent

		$\alpha_{CO2,rich}$ (mol/mol)	$\alpha_{CO2,lean}$ (mol/mol)	E_{pump} (GJ/t_{CO2})	$-E_{condenser}$ (GJ/t_{CO2})	$E_{LVC/RVC,compressor}$ (GJ/t_{CO2})	E_{regen} (GJ/t_{CO2})	E_{regen} savings /conv. conf. (%)
CONV. conf.	MEA	0.51	0.21	$1.57\ 10^{-2}$	1.94	-	3.36	-
	PZ	0.73	0.18	$1.56\ 10^{-2}$	0.93	-	3.14	-
	MDEA+PZ	0.78	0.17	$1.58\ 10^{-2}$	0.59	-	2.75	-
RSR conf.	MEA	0.51	0.27	$1.57\ 10^{-2}$	1.89	-	3.07	8.5
	PZ	0.71	0.23	$1.58\ 10^{-2}$	1.04	-	3.08	1.9
	MDEA+PZ	0.79	0.17	$1.56\ 10^{-2}$	0.64	-	2.66	3.3
SSF conf.	MEA	0.50	0.22	$1.57\ 10^{-2}$	1.02	-	3.22	4.2
	PZ	0.70	0.33	$1.57\ 10^{-2}$	0.49	-	2.99	4.7
	MDEA+PZ	0.72	0.26	$1.57\ 10^{-2}$	0.23	-	2.49	9.5
LVC conf.	MEA	0.51	0.20	$1.58\ 10^{-2}$	0.91	$8.28\ 10^{-2}$	2.91	13.4
	PZ	0.67	0.45	$2.67\ 10^{-2}$	0.82	$65.0\ 10^{-2}$	2.57	18.2
	MDEA+PZ	0.74	0.27	$2.19\ 10^{-2}$	0.60	$37.0\ 10^{-2}$	2.43	11.5
RVC conf.	MEA	0.47	0.25	$1.58\ 10^{-2}$	1.52	$13.6\ 10^{-2}$	2.95	12.1
	PZ	0.53	0.27	$2.70\ 10^{-2}$	0.73	$65.0\ 10^{-2}$	2.63	16.2
	MDEA+PZ	0.75	0.27	$2.15\ 10^{-2}$	0.48	$29.0\ 10^{-2}$	2.39	13.1

In terms of CO_2 loading, Tab. 9 indicates that for all the solvents, the process configuration does not have a significant impact on the α_{CO2} except for PZ 40 wt.% applying RVC configuration, its rich CO_2 loading being reduced from 0.73 mol CO_2/mol PZ (conventional process) to 0.53 mol CO_2 /mol PZ (with RVC). This decrease is justified by the fact that the optimum (L/G) ratio in such case is higher than with other configurations, leading to a decrease of the CO_2 cyclic capacity and thus of the rich CO_2 loading (the CO_2 absorption rate being kept at 90%). Comparing the different solvents, PZ-based solutions have higher $\alpha_{CO2,rich}$ values (up to almost 0.8 mol CO_2/mol amine) that MEA 30 wt.% (around 0.5 mol CO_2/mol amine). Concerning the $\alpha_{CO2,lean}$ values, quite logically, thanks to alternative configurations, the solutions can be less regenerated (higher $\alpha_{CO2,lean}$ values) leading to a decrease of E_{regen}. In the case of PZ 40 wt.% applying LVC configuration, the $\alpha_{CO2,lean}$ is particularly high (0.45 mol CO_2/mol PZ) in comparison with other solvents.

Looking to the energy consumptions in Tab. 9, it can be seen that the pumping energy (E_{pump}) is very low (from $1.5\ 10^{-2}$ to $2.7\ 10^{-2}$ GJ/t_{CO2}) in comparison with the other energy demands. The energy used for compression in LVC and RVC configurations is more significant than E_{pump} (from $8\ 10^{-2}$ to $65\ 10^{-2}$ GJ/t_{CO2}) but it is clearly lower than E_{regen} (from 2 to 3 GJ/t_{CO2}). Focusing on the compression energy, naturally, $E_{LVC/RVC,compressor}$ is higher with PZ-based solvents due to the operating regeneration pressure (600 kPa) allowing a higher Δp (500 kPa) than with MEA 30 wt.% (100 kPa). Concerning the condenser cooling energy ($E_{condenser}$), it is lower with PZ-based solvents (less than 1 GJ/t_{CO2} with conventional configuration) than with MEA 30 wt.% (almost 2 GJ/t_{CO2} with conventional configuration). This cooling demand is significantly reduced with the use of the other process configurations, especially with the SSF one using PZ-based solvents (< 0.5 GJ/t_{CO2}).

Comparing finally the E_{regen} values predicted for the different solvents and process configurations indicated in Tab. 9 and represented on Fig. 9, it is confirmed that for all the solvents, the LVC and RVC configurations (heat pumps modifications) lead to the higher energy savings in comparison with the conventional configuration, the regeneration energy of all the solvents using LVC or RVC configurations becoming lower than 3 GJ/t_{CO2}.
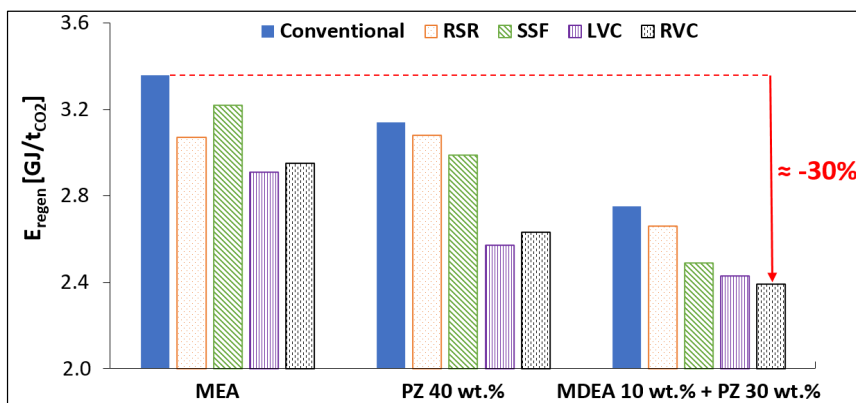

Fig. 9. E_{regen} optimum value as a function of the configuration for the three solvents considered

Indeed, obtaining such low values of E_{regen} with MEA 30 wt.% is not conventional and it can be partially linked to the flue gas considered in the present study (coming from a cement plant) which contains more CO_2 (y_{CO2} equal to 20 vol.%) than a power plant considered in other studies. Regarding the different solvents, it can be pointed out that the E_{regen} values with PZ-based solvents are lower in comparison with MEA 30 wt.%. Globally, the lowest regeneration energy was obtained with MDEA 10 wt.% + PZ 30 wt.% considering RVC configuration, namely 2.39 GJ/t_{CO2}, which corresponds to energy savings of 13% in comparison with the conventional configuration (using the same solvent). The energy savings linked to RSR and SSF modifications were lower (between 2% and 10% energy saving). Taking MEA 30 wt.% results with the conventional configuration (3.36 GJ/t_{CO2}) as reference, E_{regen} is thus reduced by almost 30% thanks to the implementation of another process configuration (RVC) and using an adequate solvent (MDEA+PZ blend).

4. Conclusion and perspectives

To reduce the CO_2 capture costs specifically for the application in the cement industry, the present work focused on Aspen Hysys™ simulations of different process configurations of the absorption-regeneration CO_2 capture process using amine based solvents (MEA 30 wt.%, PZ 40 wt.% and MDEA 10 wt.% + PZ 30 wt.%). As case study, the flue gas considered in the simulations corresponded to the Norcem Brevik Cement plant flue gas and the installation simulated was based on the CASTOR/CESAR European Projects pilot. In order to be representative of the three categories of process modifications (absorption enhancement, heat integration and heat pump effect), four process modifications were investigated in the present study, precisely RSR (Rich Solvent Recycle), SSF (Solvent Split Flow), LVC and RVC (Lean and Rich Vapor Compression). The purpose of the works was to carry out, for each configuration and solvent, a systematic parametric study on operating parameters ((L/G) ratio, split ratios, flash pressures, etc.) and determining the operating conditions leading to a minimum of the solvent regeneration energy. The simulations highlighted that the heat pump modifications LVC and RVC lead to the higher energy savings (from 11% to 18% depending on the solvent) while also reducing significantly the condenser cooling energy. Comparing the different solvents, MDEA 10 wt.% + PZ 30 wt.%, and applying RVC configuration, gives E_{regen} equal to 2.39 GJ/t_{CO2}, corresponding to a decrease of almost 30% in comparison with the base case configuration with MEA 30 wt.%. Such low regeneration energy values can be partially related to higher CO_2 content of the cement plant flue gases in comparison with power plants.

In our future works, other configurations will be also envisaged such as the combination of two configurations (for example RSR/SSF and LVC/RVC, or the combination of RVC/LVC with an Intercooled Absorber (ICA)). In addition to the interest in terms of operation expenditure (OPEX), the consequence in terms of capital expenditure (CAPEX) will be investigated in order to evaluate more precisely the global economic interest of using alternative process configurations for the application of the post-combustion CO_2 capture in the cement industry.

Acknowledgements

References

[1] Wang S., Xu Z. Absorption-Based Post-Combustion Capture of Carbon Dioxide , 1st Edition – Edited by P. Feron. Chap. 9, 201-223, 2016.

[2] Le Moullec Y., Neveux T., Al Azki A., Chikukwa A., Hoff K.A.. Process modifications for solvent-based post-combustion CO2 capture. *Int. J. Greenhouse Gas Control*, 31, 96–112, 2014.

[3] Bjerge L-M., Brevik P. CO_2 Capture in the Cement Industry, Norcem CO_2 Capture Project (Norway). *Energy Procedia*, 63, 6455-6463, 2014.

[4] Knudsen J.N., Jensen J.N., Vilhelmsen P-J., Biede O. Experience with CO_2 capture from coal flue gas in pilot-scale: Testing of different amine solvents. *Energy Procedia*, 1, 783-790, 2009.

[5] Dubois L., Thomas D. Comparison of various configurations of the absorption-regeneration process using different solvents for the post-combustion CO_2 capture applied to cement plant flue gases. Submitted for publication in *Int. J. Greenhouse Gas Control*, 2016.

[6] Zhang Y., Chen H., Chen C.-C., Plaza J.M. Dugas R., Rochelle G.T., 2009. Rate-Based Process Modeling Study of CO_2 Capture with Aqueous Monoethanolamine Solution. *Ind. Eng. Chem. Res.*, 48, 9233-9246.

[7] Song Y., Chen C.-C. Symmetric Electrolyte Nonrandom Two-Liquid Activity Coefficient Model. *Ind. Eng. Chem. Res.*, 48, 7788-7797, 2009.

[8] Zhang Y., Chen C.-C.. Thermodynamic Modeling for CO_2 Absorption in Aqueous MDEA Solution with Electrolyte NRTL Model. *Ind. Eng. Chem. Res.*, 50, 163-175, 2011a.

[9] Zhang Y., Que H., Chen C.-C. Thermodynamic Modeling for CO_2 Absorption in Aqueous MEA Solution with Electrolyte NRTL Model. *Fluid Phase Equilibria*, 311, 68-76, 2011b.

[10] Knudsen J.N., Jensen J.N., Vilhelmsen P-J., Biede O., 2009. Experience with CO_2 capture from coal flue gas in pilot-scale: Testing of different amine solvents. *Energy Procedia*, 1, 783-790.

[11] Le Moullec Y., Neveux T. Absorption-Based Post-Combustion Capture of Carbon Dioxide, 1st Edition – Edited by P. Feron. Chap. 13, 305-340, 2016.

[12] Sanchez Fernandez E., Bergsma E.J., de Miguel Mercader F., Goetheer E.L.V, Vlugt T.J.H. Optimisation of lean vapour compression (LVC) as an option for post-combustion CO_2 capture: Net present value maximization. *Int. J. Greenhouse Gas Control*, 11S, S114–S121, 2012.

[13] van der Ham L.V., Romano M.C., Kvamsdal H.M., Bonalumi D., van Os P., Goetheer E.L.V. Concentrated aqueous piperazine as CO_2 capture solvent: Detailed evaluation of the integration with a power plant. *Energy Procedia*, 63, 1218 – 1222, 2014.

[14] Freeman S.A., Dugas R., Van Wagener D.H., Nguyen T., Rochelle G.T. Carbon dioxide capture with concentrated, aqueous piperazine. *Int. J. Greenhouse Gas Control*, 4, 119–124, 2010.

[15] Mudhasakul S., Ku H-M., Douglas P.L. A simulation model of a CO_2 absorption process with methyldiethanolamine solvent and piperazine as an activator. *Int. J. Greenhouse Gas Control*, 15, 134–141, 2013.

[16] Roh K., Lee J.H., Gani R., A methodological framework for the development of feasible CO_2 conversion processes. *Int. J. Greenhouse Gas Control*, 47, 250–265, 2016.

[17] Gervasi J., Dubois L., Thomas D. Simulation of the Post-combustion CO_2 Capture with Aspen Hysys^{TM} Software: Study of Different Configurations of an Absorption-regeneration Process for the Application to Cement Flue Gases. *Energy Procedia*, 63, 1018-1028, 2014.